ACOUSTIC PROPERTIES AND THEIR DEPENDENCE ON POROSITY, MINERALOGY, AND SATURATION: APPLICATIONS TO FIELD-SCALE MEASUREMENTS

Dominique Marion and Diane Jizba
Elf Aquitaine, Pau, France

Abstract A laboratory study was conducted to investigate the influence of porosity, mineralogy (shaliness), partial saturation and frequency on P and S velocities. Acoustic measurements were conducted at sonic (20-50 kHz) and ultrasonic (300-700 kHz) frequencies on shaly sandstones covering a range of porosities from 1 to 14% and clay content from 0 to 50%. To quantify the influence of mineralogy on acoustic properties, elastic moduli of the mineral phase were measured directly from drained, unjacketed mechanical tests.

Results of this study show that most of the scatter in the velocity-porosity relations is attributed to mineralogy and may be accounted for from the knowledge of shaliness. This is especially true for shear velocity which is strongly affected by clay content. For partial saturation we find that the velocity versus saturation relation is not modeled adequately using the Gassmann theory (1951). This is due to heterogeneities in the saturation at the microscopic scale and velocity dispersion due to intrinsic attenuation. We propose a relationship that takes into account saturation heterogeneities and local flow dispersion mechanism to describe the velocity dependence on partial saturation.

Results of this laboratory study were applied to the interpretation of sonic measurements in terms of porosity and saturation.

INTRODUCTION

Petrophysical and lithological properties such as porosity, saturation, shaliness have a marked impact on acoustic properties of rocks. Hence, there has been recently a strong incentive to use new geophysical techniques to invert such properties from seismic or sonic measurements for reservoir characterization purposes. However, because of the complexity of the structure of the pore space and fluid-solid interactions in rocks, there is no simple theoretical relationship that could be used for an accurate interpretation for sonic and seismic data. Therefore, there is the need to calibrate quantitative interpretations of velocities or impedances using core measurements that allow to investigate the influence of petrophysical and lithological properties under controlled conditions of pressure, temperature, fluid type, and frequency.

In this paper we illustrate through a case study, the use of core measurements in the calibration of sonic interpretation. We first present the results from core analysis. More specifically, we investigate the effect of porosity, shaliness and saturation that vary from one well to another and may affect sonic and seismic responses. We then apply the results from core measurements to sonic interpretation.

EXPERIMENTAL PROCEDURES

In this shaley sand reservoir, observations between wells indicate variability in porosity, mineralogy, shaliness, and saturation that may affect seismic measurements. Hence in this laboratory study, we investigated more specifically the influence of these parameters on acoustic measurements. Thirteen core samples were selected from representative reservoir facies with porosity ranging from 0.9 to 14% and clay content ranging from 0 to 50%.

Compressional and shear velocities were measured using the pulse transmission technique (Birch 1960) on dry and brine saturated samples at various confining pressures up to a maximum of 37 MPa and pore pressure of 2 MPa. Central frequencies for P and torsional S transducers were 500 KHz. P velocity was also measured at ambient conditions of pressure and temperature on dry, brine saturated, and

partially saturated samples using 50 kHz and 500 kKz center frequency transducers.

Porosity and grain density were measured on all samples at ambient conditions. Porosity at reservoir conditions was measured from the amount of brine expelled from the sample under increasing confining pressure.

Mineralogy was estimated from point counting on thin section and X-ray diffraction semi-quantitative analysis.

Elastic properties of mineral aggregates were measured using a drained unjacketed mechanical test. In this experiment, the sample was immersed in the confining fluid and volumetric strain was measured as a function of stress (up to 40 MPa) using strain gauges. Bulk modulus was then computed from the slope of the stress-strain curve.

RESULTS FROM CORE MEASUREMENTS

A summary of data collected at 35 MPa is given in Table 1. In this data set Poisson's ratio, bulk, and shear moduli, γ, K and G respectively, were computed from the relations

$$\gamma = \frac{(V_p/V_s)^2 - 2}{2((V_p/V_s)^2 - 1)} \tag{1}$$

$$K = \rho\left(V_p^2 + \frac{4}{3}V_s^2\right) \tag{2}$$

$$G = V_s^2 \tag{3}$$

where Vp, Vs, and ρ are the P-velocity, the S-velocity and the bulk density respectively.

Table 1 Acoustic* and Petrophysical Data

S_g=1					S_w=1				
V_p (km/s)	V_s (km/s)	K (GPa)	G (GPa)	ν	V_p (km/s)	V_s (km/s)	K (GPa)	G (GPa)	ν
4.475	3.099	18.46	24.56	.039	5.156	3.153	35.08	26.18	.201
4.516	2.974	21.37	21.97	.117	4.926	3.016	31.64	23.71	.200
4.351	2.998	17.57	22.71	.048	4.879	3.023	30.45	23.90	.189
4.265	2.964	15.29	20.77	.033	4.689	2.893	27.21	21.07	.193
4.490	3.071	19.49	24.22	.061	5.080	3.088	34.50	25.22	.207
4.139	2.792	15.66	18.11	.083	4.517	2.763	25.49	19.04	.201
4.424	3.041	18.17	23.21	.052	4.903	2.991	31.74	23.42	.204
4.388	2.817	22.75	20.83	.149	4.853	2.847	34.21	21.76	.238
4.645	3.050	23.71	24.06	.121	5.219	3.119	37.10	25.32	.222
4.083	2.696	16.33	17.00	.113	4.576	2.723	27.50	18.45	.226
4.312	2.887	18.36	20.44	.094	4.867	2.949	31.06	22.34	.210
4.091	2.704	16.85	17.65	.112	4.548	2.646	29.01	17.88	.244
4.581	2.825	25.60	19.76	.193	-	-	-	-	-

ϕ	kg (md)	ρ_{ma} (g/cm^3)	V_{sh}	K_{ma} (GPa)
.064	1.16	2.74	.10	42.3
.106	4.42	2.79	.00	48.5
.063	.05	2.72	.03	43.4
.117	10.21	2.71	.00	41.8
.047	.01	2.72	.10	41.8
.132	13.25	2.71	.07	40.9
.086	.47	2.77	.11	37.9
.027	< .001	2.73	.34	32.8
.048	.01	2.72	.10	41.8
.113	1.95	2.67	.16	40.0
.075	.60	2.70	.00	42.7
.089	.18	2.70	.09	39.1
.009	< .001	2.72	.50	31.5

* Measurements made at 35 MPa effective pressure.
- Not measured.

INFLUENCE OF POROSITY AND SHALINESS

The cross-plot in Figure 1 shows the combined effect of porosity, saturation and shaliness on velocity in this North sea shaley sand reservoir. At a given saturation (Sg=1 and Sw=1), the scatter in the velocity-porosity relationship may be attributed primarily to the effect of clay content. From statistical analysis, we find a linear relationship between velocity, porosity and clay content comparable to Han et al. relations (1986) but with slightly different coefficients.

For a gas reservoir at 35MPa, we find for P and S velocities in km/s:

$$V_p = 4.82 - 5.02\phi - 0.597V_{sh} \quad (4)$$

$$V_s = 3.26 - 3.03\phi - 0.892V_{sh} \quad (5)$$

For a brine saturated reservoir at 35MPa:

$$V_p = 5.46 - 6.29\phi - 1.10V_{sh} \quad (6)$$

$$V_s = 3.32 - 3.62\phi - 0.952V_{sh} \quad (7)$$

where ϕ, and V_{sh} are the porosity and clay content respectively. We note from equations 4-7, that to first order the effect of porosity on P and S velocities is comparable, S velocities are insensitive to saturation, and the effect of clay is most important for shear velocities.

We find, looking at elastic moduli (Figure 2), that clay affects mostly shear modulus and has only a limited influence on bulk modulus. Bulk modulus in contrast, is strongly influenced by saturation.

INFLUENCE OF SATURATION

We notice on Figure 1 and from the relations 4 to 7 that saturation affects mostly compressional velocity and has a limited influence on shear velocity. This behavior can be explained theoretically using Gassmann's equations that relate the saturated rock elastic moduli to the dry rock moduli

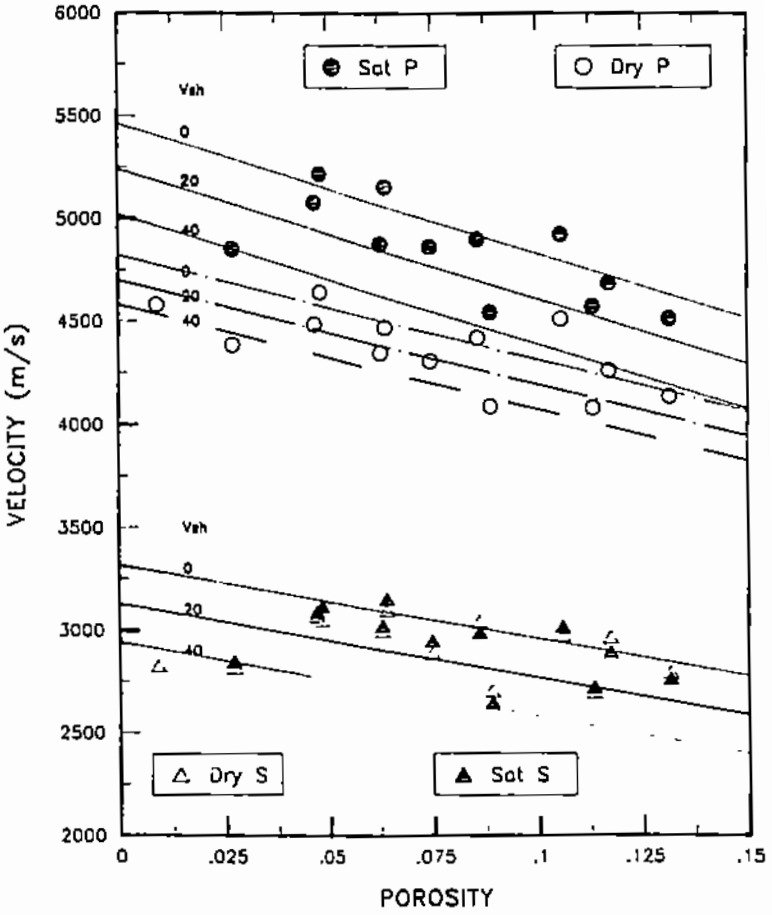

Figure 1: Influence of saturation and clay on P and S velocities for a North sea gas reservoir.

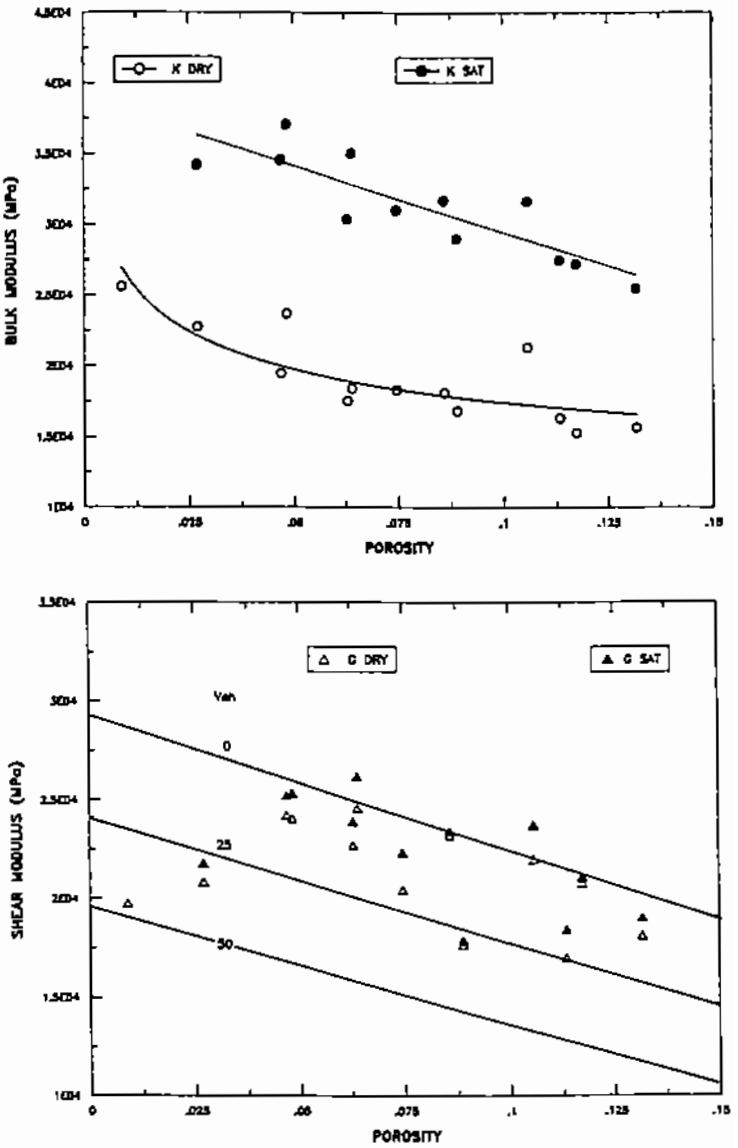

Figure 2: Relation between bulk and shear modulus and porosity. Apparent dispersion between shear modulus and porosity is attributed to shaliness. Bulk modulus exhibits strong dependence on saturation.

$$K_{sat} = K_{dry} + \frac{(1 - K_{dry}/K_{ma})^2}{\frac{\phi}{K_{fl}} + \frac{(1-\phi)}{K_{ma}} - \frac{K_{dry}}{K_{ma}^2}} \tag{8}$$

$$G_{sat} = G_{dry} \tag{9}$$

where Ksat, Kdry, Kma, Kfl are the bulk moduli of the saturated rock, the dry rock, the mineral grains, and the pore fluid respectively and Gsat and Gdry are the shear moduli of the saturated and the dry rock respectively.

Using input parameters listed in Table 1, these relationships were used to predict the effect of saturation on velocities. Figure 2 shows a comparison between Gassmann's predictions and the velocity data. We can notice that Gassmann's prediction underestimates the increase in velocity from a dry to a brine saturated rock.

The discrepancy between ultrasonic velocity data on fluid saturated rocks and the Gassmann low frequency approximation may represent frequency dispersion (Winkler, 1985, 1986) that is primarily related to grain-scale microscopic flow field as experiments (Murphy et al., 1984; Wang and Nur, 1988) and models (O'Connell and Budiansky, 1974,1977; Mavko and Nur, 1979; Mavko and Jizba, 1991) suggest: In the low frequency regime described by the Gassmann model, when a wave propagates in a fluid saturated rock, pore fluid can flow easily from one pore to another and the frame modulus is in a drained state. In contrast, at high frequencies, viscous effects coupled with heterogeneities in the geometry and the compressibility of the pore space induce local pore pressure gradients between the thin and large pores. The frame is then in a partially drained state also called "unrelaxed" and is stiffer than in the low frequency regime.

In an attempt to model and predict velocity dipersion between high frequency ultrasonic measurements and low frequency seismic velocities, we used the formulation proposed by Mavko and Jizba (1991) to describe velocity dispersion due to grain-scale local flow

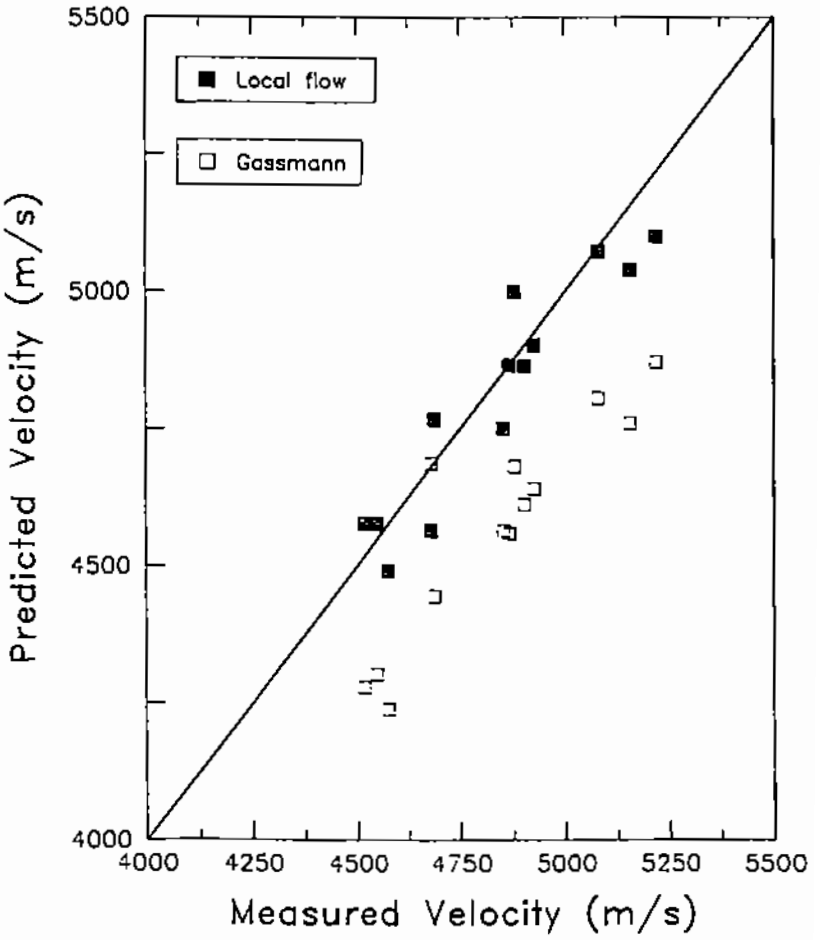

Figure 3: Cross-plot of predicted vs. measured velocities using Gassmann (low frequency) and Local Flow (high frequency) predictions for brine-saturated rocks.

effects. As a first order approximation, we considered that the high frequency unrelaxed frame modulus Kuf may be estimated from the dry frame modulus at high confining pressure $K_{h\sigma}$. The high frequency limit for compressional velocity is then obtained using Gassmann's relation where the frame modulus Kdry is replaced by the unrelaxed modulus at high stress $K_{h\sigma}$. At high stress, the weakening effect of cracks and compliant pores may be neglected, and the high pressure frame modulus for sandstones may be estimated using the modified Voigt average (Nur, A., personal communication).

$$K_{h\sigma} = \left(1 - \frac{\phi}{\phi_c}\right) K_{ma} \qquad (10)$$

where ϕ_c is the critical porosity at the transition from a suspension to a load-bearing frame which is typically of the order of 0.4 for sedimentary rocks (Marion et Nur, 1988).

We notice in Figure 3 that most of the dispersion between high frequency velocity data and Gassmann's low frequency approximation may be accounted for using the local flow model.

INFLUENCE OF PARTIAL SATURATION

To investigate the possible effect of invasion and variations in fluid saturation on velocity measurements, velocity was measured at partial saturation on a few samples during drainage (drying) and spontaneous imbibition. In addition, compressional velocity was measured at sonic (30 kHz) and ultrasonic (500 kHz) frequencies to investigate velocity dispersion between laboratory and well-log measurements.

In Figure 4, experimental data were compared with Gassmann's equations for partial saturation. Note that in Gassmann's equations applied to partial saturation, the fluid distribution is considered as homogeneous at the scale of the pore and bulk modulus of the fluid phase is:

$$K_{fl} = \left(\frac{S_w}{K_{brine}} + \frac{1 - S_w}{K_{air}}\right)^{-1} \qquad (11)$$

We note from Figure 4:

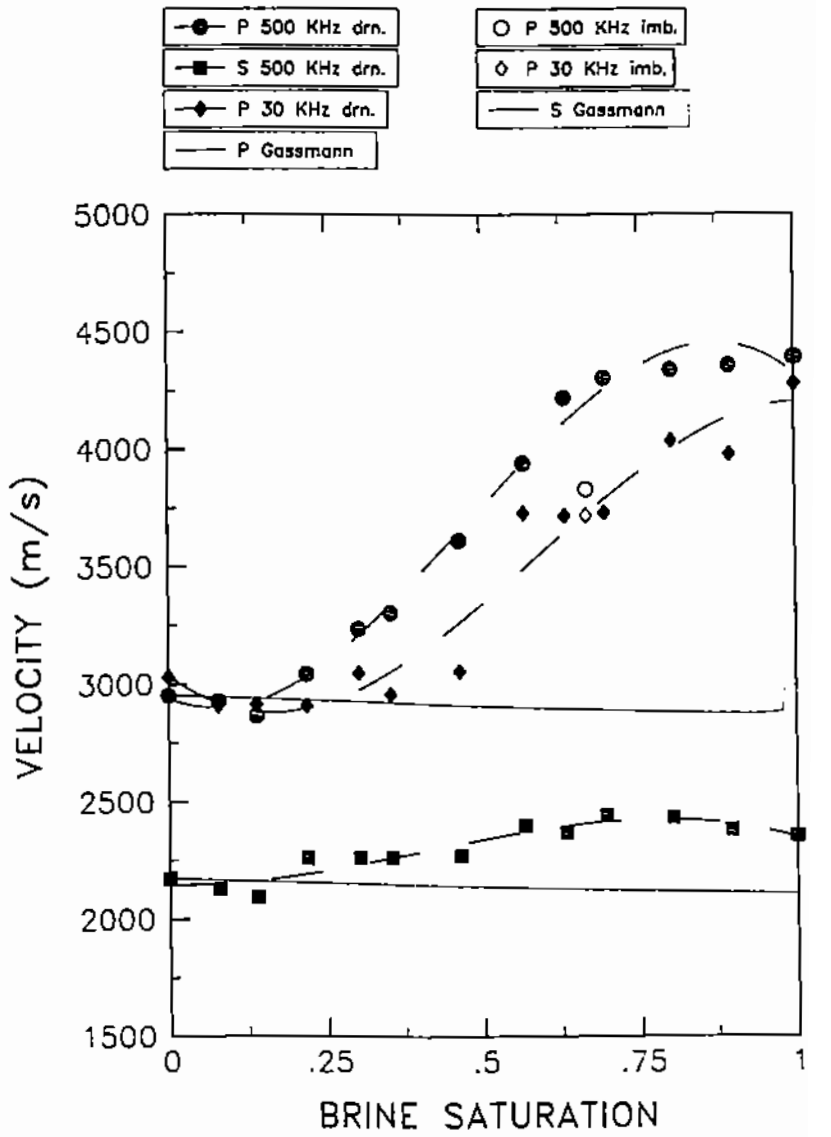

Figure 4: P and S velocity vs. partial saturation at sonic (30 kHz) and ultrasonic (500 kHz) frequencies. The difference between measurements and the Gassmann prediction is attributed to saturation heterogeneities at the pore scale and local flow frequency dispersion.

1. Velocity dispersion as shown by the difference between data and Gassmann's prediction at Sw=1.

2. Saturation is heterogeneous at the pore scale as shown by the distinct trends between data and Gassmann's model.

3. During drying, saturation is heterogeneous at the centimetric scale as shown by the discrepancy between sonic and ultrasonic data that "average" differently heterogeneities.

To model this data set at sonic frequencies we consider that between Sw=0 and Sw=Swi=.3, gas is present in each pore and data are modeled using Gassmann's relation. For Sw greater than Swi, pores are either filled completely with liquid and behave as unrelaxed or they are at Sw and behave as relaxed (Gassmann behavior). Hence bulk modulus can be written as

$$K = \left(\frac{1 - S_w}{1 - S_{wi}}\right) K_{gassmann} + \left(\frac{S_w - S_{wi}}{1 - S_{wi}}\right) K_{unrelaxed} \qquad (12)$$

COMPARISON BETWEEN LOG AND CORE DATA

To apply the laboratory results to well-log interpretation we first verify the agreement between core and log data.

Figure 5 shows a comparison between core data at in situ stress conditions and array sonic data. We note in particular that the P-wave travel time and the Vp/Vs ratio fall in-between the core values measured at Sw=1 and Sg=1.

In Figure 6, comparable trends are observed for P and S impedance from core measurements and well-logs. These observations were used to analyze the sensitivity of impedance to porosity and saturation. On Figure 6, we note that the dispersion between impedance and porosity may be attributed primarily to saturation for P waves and shaliness for S waves.

APPLICATION TO WELL LOG INTERPRETATION

Once the core data are calibrated with well-log data, the rock physics relationships established using core measurements can be used for

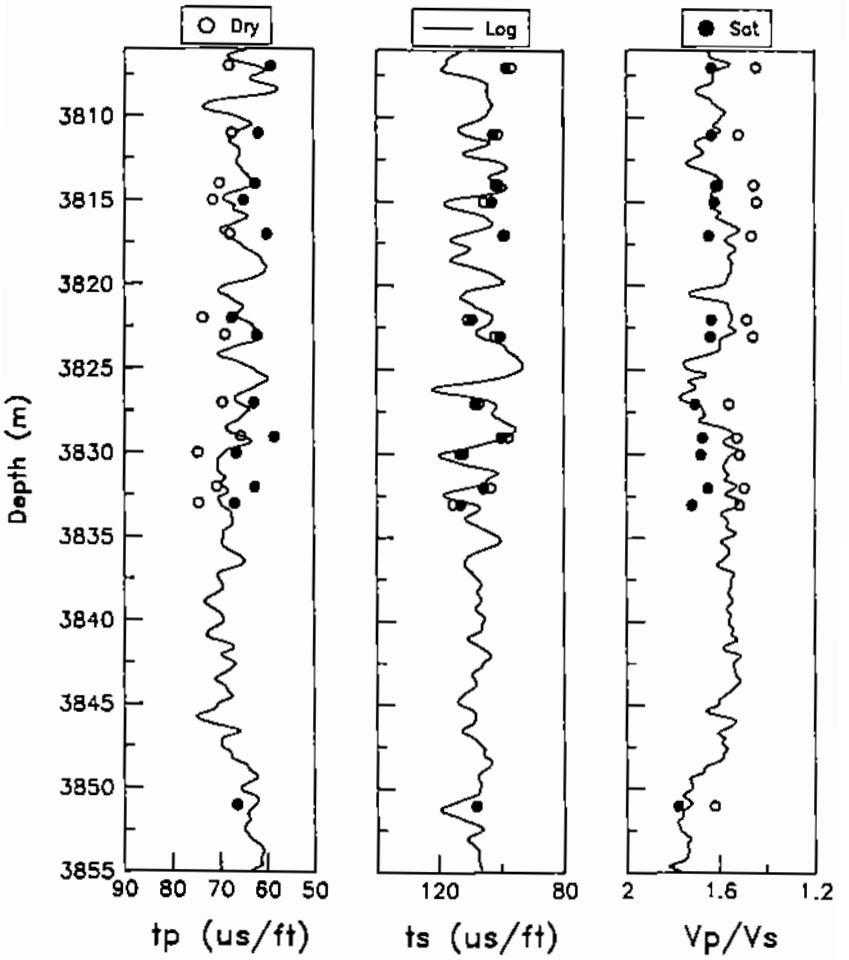

Figure 5: Comparison of well-log array sonic measurements and core measurements of P- and S-wave travel time and Vp/Vs ratio.

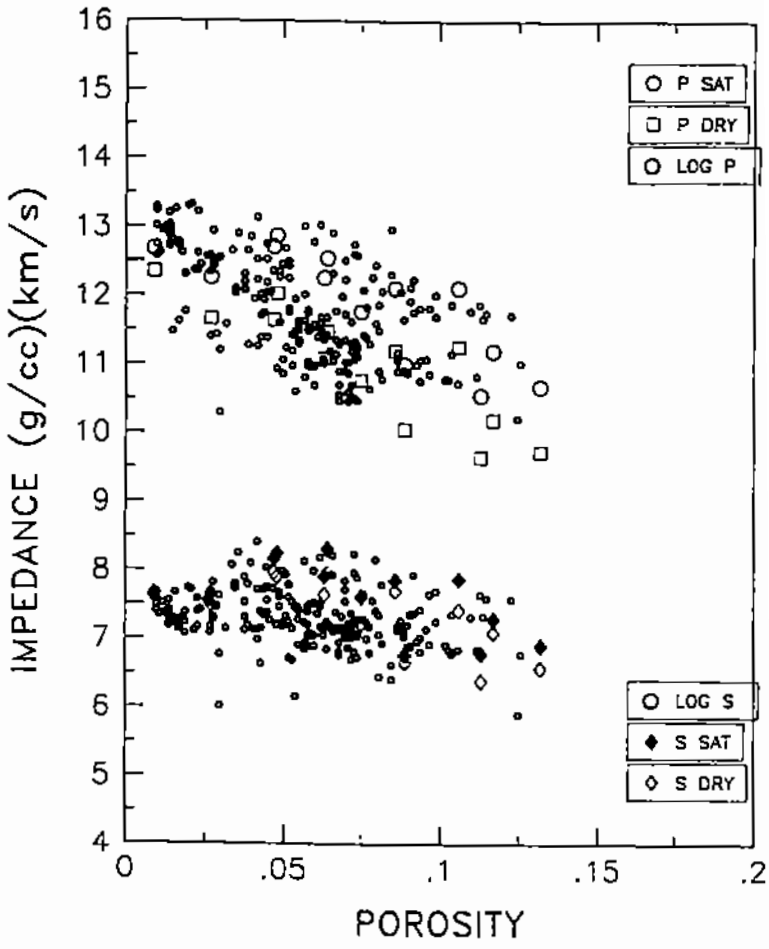

Figure 6: Cross plot comparison between P and S impedance and porosity for core and well log measurements.

the quantitative interpretation of sonic-log data. The laboratory results were applied to well-log data to the estimation of porosity and saturation (Figure 7 and 8).

Figure 7 shows an example of a porosity log generated from the sonic log-S. This log is calculated using equation 5 established from laboratory measurements and clay content, estimated from gamma ray. The porosity log calculated from the sonic log-S is in good agreement with core data and gives comparable results to porosity calculations based on neutron-density methods. An advantage of using the log-S for porosity estimation is that it is unaffected by invasion effects often encountered in gas wells.

A second application to sonic-log data deals with the delineation of gas-water zones. The laboratory results were used to calculate a pseudo Vp/Vs log at irreducible water saturation, Sw=Swi (approximately 30 percent), and at full brine-saturation, Sw=1. Comparison of the measured Vp/Vs log and the simulated logs (Figure 8) indicates the presence of gas where the log is close to the pseudo-log at Sw=Swi and water zones where the log is close to the pseudo-log at Sw=1. These observations were confirmed from independent observations using neutron and density crossover.

In this section we have shown that once laboratory measurements are calibrated with well-log data, they can be used for the quantitative interpretation of sonic data in terms of porosity and saturation. Other applications include modelling at seismic frequencies the effect of porosity and saturation and the interpretation of AVO data based on the Vp/Vs ratio.

SUMMARY

We present a laboratory study designed to investigate the influence of rock and fluid parameters on acoustic properties. Acoustic measurements were conducted at sonic (20-50 kHz) and ultrasonic (300-700 kHz) frequencies on shaly sandstones covering a range of porosities from 1 to 14% and clay content from 0 to 50%. To quantify the influence of mineralogy on acoustic properties, elastic moduli of the mineral phase were measured directly from drained, unjacketed mechanical tests.

The laboratory results indicate that the acoustic behavior of this

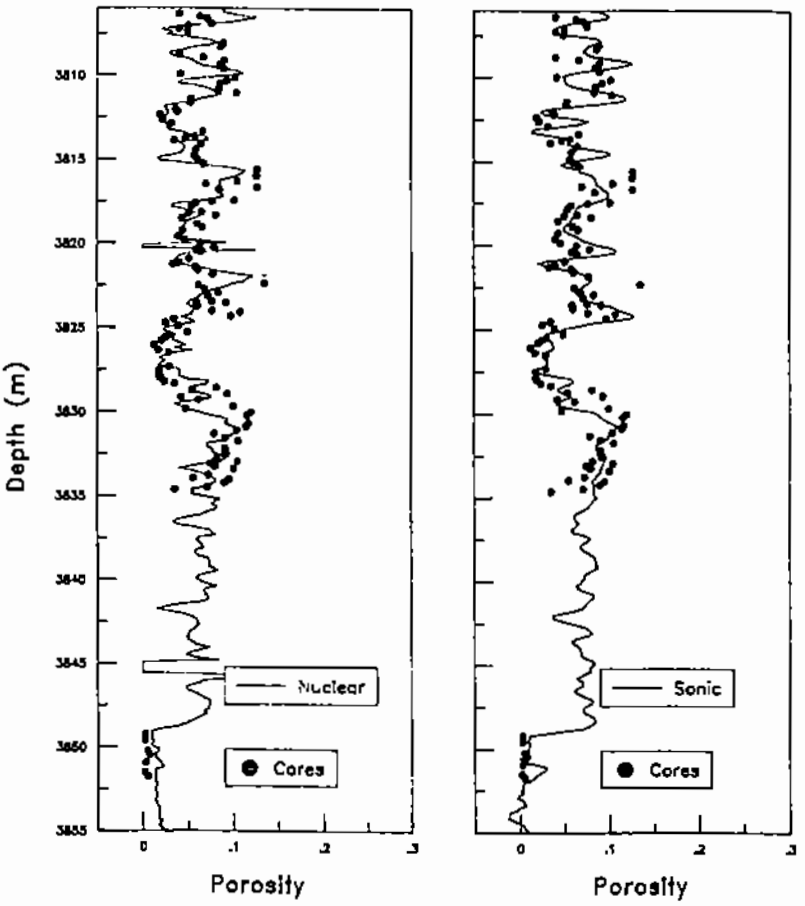

Figure 7: Porosity log calculated using S-wave velocity, clay content from gamma ray, and equation (5). Good correspondence with core measurements and porosity estimate from neutron - density logs.

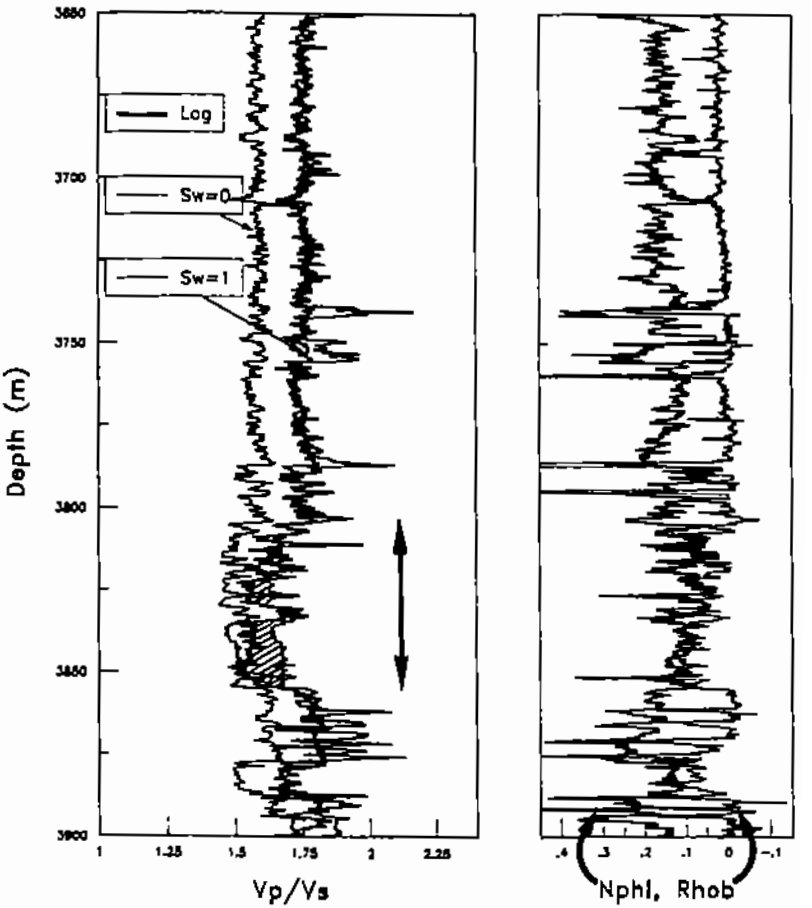

Figure 8: Delineation of gas zones by the relative position of measured Vp/Vs ratio with respect to the calculated logs for Sw=Swi and Sw=1.

sandstone is controlled primarily by porosity, saturation, and clay content. For partial saturation we find that the velocity versus saturation relation is not modeled adequately using Gassmann theory. This is due to heterogeneities of the saturation at the microscopic scale and velocity dispersion due to intrinsic attenuation. A relation was proposed that more accurately describes the velocity dependence on partial saturation.

The laboratory results, calibrated on core measurements and validated at the well-log scale, permitted to interpret sonic P- and S-logs quantitatively in terms of porosity and saturation.

REFERENCES

BIRCH, (1960) The velocity of compressional waves in rocks to 10 kilobars, 1: J. Geophys. Res., 65 1083-1102.

GASSMANN, F., (1951) Elastic waves through a packing of spheres: Geophysics, 16, 673-685.

HAN, D., NUR, A., and MORGAN, D. (1986) Effect of porosity and clay content on wave velocity in sandstones.Geophysics, 51, 2093-2107.

MARION D. P, and NUR, A., (1988) Percolation of electrical and elastic properties of granular materials at the transition from a suspension to a loose random packing, ETOPIM2 proceedings, Physica A.

MAVKO, G. M., and NUR, A. (1979) Wave attenuation in partially saturated rocks, Geophysics, 44, 161-178.

MAVKO, G.M., and JIZBA, D. (1991) Estimating grain-scale effects on bulk and shear dispersion in rocks: Geophysics, 56, 1940-1949.

MURPHY, W. F., WINKLER, K. W., and KLEINBERG, R. (1984) Contact microphysics and viscous relaxation in sandstones, in Physics and Chemistry of Porous media, edited by D. L. Johnson and P.N. Sen, American Institute of Physics, New York.

O'CONNELL, R.J., BUDIANSKY, B. (1974) Seismic velocities in dry and saturated cracked solids: J. Geophys. Res., 79, 5412-5426.

O'CONNELL, R.J., BUDIANSKY, B. (1977) Viscoelastic properties of fluid saturated cracked solids. J. Geophys. Res., 76, 2022-2034

WANG Z,. and NUR, A. (1988) Velocity dispersion and the "local flow" mechanism in rocks, 58th Ann. Internat. Mtg. Soc. Explor. Geophys., Expanded Abstracts, 928-930.

WINKLER, K. (1985) Dispersion analysis of velocity and attenuation sandstones. J. Geoph. Res., 88, 9493-9499.

WINKLER, K. (1986) Estimates of velocity dispersion between seismic and ultrasonic frequencies: Geophysics, 51, 183-189.

Capillary Pressure